Int J Adv Manuf Technol (2016) 85:2125–2138
DOI 10.1007/s00170-015-8248-y

ORIGINAL ARTICLE

Experimental studies on tool wear in μ-RUM process

Anil Kumar Jain[1] · **Pulak M. Pandey**[2]

Received: 15 April 2015 / Accepted: 15 December 2015 / Published online: 15 January 2016

Abstract Tool wear in micro-manufacturing process is of paramount importance to meet stringent design requirements of workpiece in a cost-effective manner. In present work, tool wear in micro-rotary ultrasonic machining (μ-RUM) has been investigated for Ø300-μm peck drilling operation. Two sets of experiments have been conducted using electroplated hollow diamond tool and borosilicate glass as workpiece to evaluate the effects of μ-RUM parameters on tool wear. In the first set, the effects of tool-based parameters like grain size and thickness of hollow tool have been studied using full factorial design and optimum tool design was obtained. In second set, the effects of process-related parameters like spindle speed, distance traverse in each stroke, table feed rate, vibration amplitude, and vibration frequency on tool wear were studied using central rotatable composite design with optimum tool designed in first step. Analysis of variance has been used to study the significance of μ-RUM factors on tool wear. After investigation and analysis of the data, it has been concluded that thickness and grain size of hollow diamond tool had an inverse effect on tool wear. Tool with 100-μm thickness and 30-μm grain size was best possible tool for minimum tool wear. It has also been found that process parameters like traverse in each stroke, vibration amplitude, vibration frequency, and spindle speed have affected tool wear, but vibration frequency was most influencing process parameter and resulted in rapid tool wear if not selected properly.

✉ Anil Kumar Jain
aniljain11in@yahoo.co.in

Pulak M. Pandey
pmpandey@mech.iitd.ac.in

[1] Advance Manufacturing Facility/Internal Fabrication facility/ Material Mechanical Entity, Vikram Sarabhai Space Centre, Indian Space Research Organization, Trivandrum, Thiruvananthapuram, Kerala, India

[2] Department of Mech Eng., IIT Delhi, India, IIT Delhi, India

Keyword Rotary ultrasonic machining · Micro-rotary ultrasonic machining · Vibration frequency · Vibration amplitude · Micro-grinding · Tool presetter · Electroplated hollow diamond tool · Borosilicate glass · Peck drilling · Specific tool wear · Tool wear

Abbreviations

μ-RUM	Micro-rotary ultrasonic machining
MEMS	Micro-electro mechanical system
USM	Ultrasonic stationary machining
RUM	Rotary ultrasonic machining
DOEs	Design of experiments
μ-grinding	Micro-grinding
rpm	Rotation per minute
SEM	Scanning election microscope

Nomenclature

α	Level of confidence interval
β_i, β_{ii}, and β_{ij}	Constant coefficients
$\in$	Error
V_e	Error variance
Y	Response variable
MS	Mean square
Seq. SS	sequential sum of squares
SS	Sum of squares
F	Fisher's value
df	Degrees of freedom
G	Specific tool wear or grinding ratio or wear ratio
d_p	Distance traverse in each stroke or depth of cut in peck drilling
f_r	Feed rate or feed (mm/min)
N	Spindle speed (rpm)
f	Vibration frequency (kHz)
A	Vibration amplitude (percent of power)

1 Introduction

Micro-rotary ultrasonic machining is rationalized version of rotary ultrasonic machining (RUM), which is widely used for machining advance ceramic materials like glass, SiC, and Al_2O_3 [1, 2]. In RUM, the diamond tool rotates as well as vibrates in axial direction. The RUM process involves material removal by hybrid action of ultrasonic stationary machining (USM) and conventional grinding [2]. In the process, accuracy and material removal rate are affected by tool wear [3, 4]. Tool wear is a complex phenomenon in USM and usually involves loss of tool volume and dulling of abrasive grains. It occurs mainly due to tool change at micro-level topography than that at tool profile [3, 4]. Tool wear is a major challenge in rotary ultrasonic machining, and it is more significant in case of micro-rotary ultrasonic machining. As size of the tool is in micro-domain, so the strength is relatively poor, hence tool wears rapidly [4]. Tool wear also occurs when any of the process parameters of μ-RUM is not selected correctly. No research work on tool wear in μ-RUM has been reported, although extensive literature on tool wear mechanism in grinding process and stationary ultrasonic machining is available. A brief review of tool wear mechanism and effect of RUM parameters have been provided in this paper.

Researchers [4–8] have reported three main types of tool wear mechanisms in grinding, i.e., attritious wear, grain fracture, and bond fracture. Attritious wear occurs when abrasive grains become dull and develop flat areas due to rubbing by workpiece material. Grain fracture refers exposure of new cutting edges after removal of abrasive fragments. Bond fracture is responsible for self-sharpening of tool and loss of shape and size. Tool wear in USM is classified as longitudinal and lateral wear as shown in Fig. 1 [3]. Tool wear in RUM is affected by a number of parameters given in Table 1. Many researchers [5–7] have reported the tool wear investigations in terms of RUM input parameters and discussed tool wear mechanism.

The effects of RUM process parameters like vibration amplitude, static pressure, and diamond concentration on specific tool wear were investigated by Markov et al. [5] on quartz glass as workpiece material. They concluded that specific tool wear increased with increase in static pressure due to greater load on the diamond grains. As vibration amplitude increased, specific tool wear reduced initially. Further increase in vibration amplitude resulted in increase of specific tool wear. As diamond concentration increased, specific tool wear first remained constant and then increased [5].

The effects of vibration frequency and grit size on specific tool wear were investigated by Pethurka et al. [5] using quartz glass as workpiece. They found that specific tool wear increased as vibration frequency increased and decreased with an increase in grit size [5].

Tool wear investigations in RUM of SiC were reported by Zeng et al. [6]. They observed the tool topography of lateral and end face before and after drilling test as shown in Fig. 2. Grains at lateral face were dislodged after 16 drilling tests. However, grains at end face were more severely dislodged than lateral face in RUM of SiC. There were two stages of tool wear reported in RUM of SiC. In first stage, attritious wear dominates, whereas in second stage, bond fracture dominates. The grain fracture which was commonly seen in metal grinding and conventional grinding of ceramic materials was not observed [6].

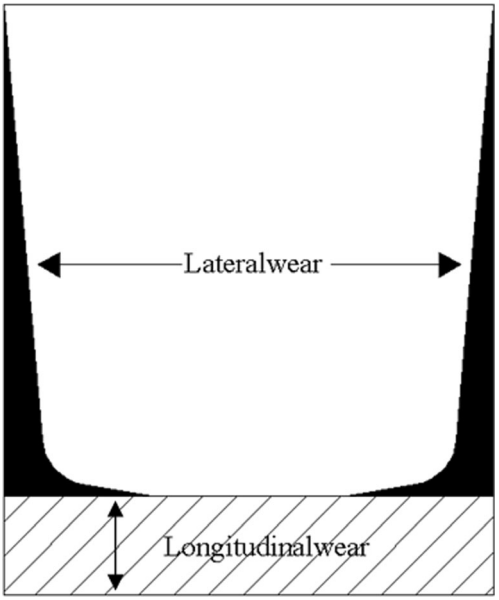

Fig. 1 Tool wear in USM [3]

Churi [7] studied wheel wear mechanism in RUM of titanium alloys for drilling operation. Different wheel wear mechanisms, namely, attritious wear, grain pullout, grain fracture, bond fracture, and catastrophic types of failures, were reported in his investigations. He studied the longitudinal tool wear with number of holes drilled for different tool geometries like tool with slot and without slot. He concluded that the tool with slots had higher wear rate than without slots [7].

It can be seen from the discussion presented above that tool wear in micro-RUM was studied for SiC, quartz glass, and titanium workpiece materials. No work has been reported for tool wear in μ-RUM. Therefore, the present work aims to investigate the effect of μ-RUM parameters on tool wear in borosilicate glass as workpiece material. These findings can be used for selecting tool and process parameters in μ-RUM for machining micro-features in brittle and hard materials.

2 Details of equipment and design of experiments

In these sections, details of experimental setup, micro-diamond tools, experiment design, and selection of process parameter and details of experiments are discussed.

Table 1 Parameters affecting tool wear in RUM

Workpiece-related parameters	Experimental setup-related parameters	Tool-related parameters	Process-related parameter
Material type (ductile/brittle)	Machine traverse, accuracy	Tool material (diamond/CBN)	Vibration amplitude
Hardness of material	Spindle type	Method (sintered/electroplated)	Vibration frequency
Young's modulus	Run out of tool	Grain size	Depth of cut
Fracture toughness	Tool length	Thickness of tool	Feed rate
Miscellaneous	Type of operation	Concentration	Spindle speed

2.1 Experimental setup

The schematic diagram of experimental setup for machining of micro-features such as Ø0.3-mm hole using μ-RUM has been shown in Fig. 3. DMG US-50 Sauer machine, shown in Fig. 4a, has been used for experiments. The equipment consists of a rotating spindle coupled to an ultrasonic transducer. The ultrasonic power supply converts conventional line voltage into 17–29.5 kHz of electrical energy. This output is fed to the piezoelectric transducer located in the spindle, and the transducer converts the electrical input into mechanical vibrations. The machine has an ultrasonic generator which can produce 300 W of peak power. The vibration amplitude is programmable in terms of percentage of ultrasonic power and can vary from 50 to 100 %. In RUM mode, the tool can attain a speed up to 6000 rpm. Figure 4b shows the drilled hole using Ø0.3 mm for the present experimentation.

2.2 Micro-diamond tools

There are four types of bonding processes used for fabricating grinding and RUM tools, namely, resin bonded, vitrified bonded, metal bonded, and electroplated [4]. Resin-bonded tools are relatively soft and less wear resistant. Vitrified-

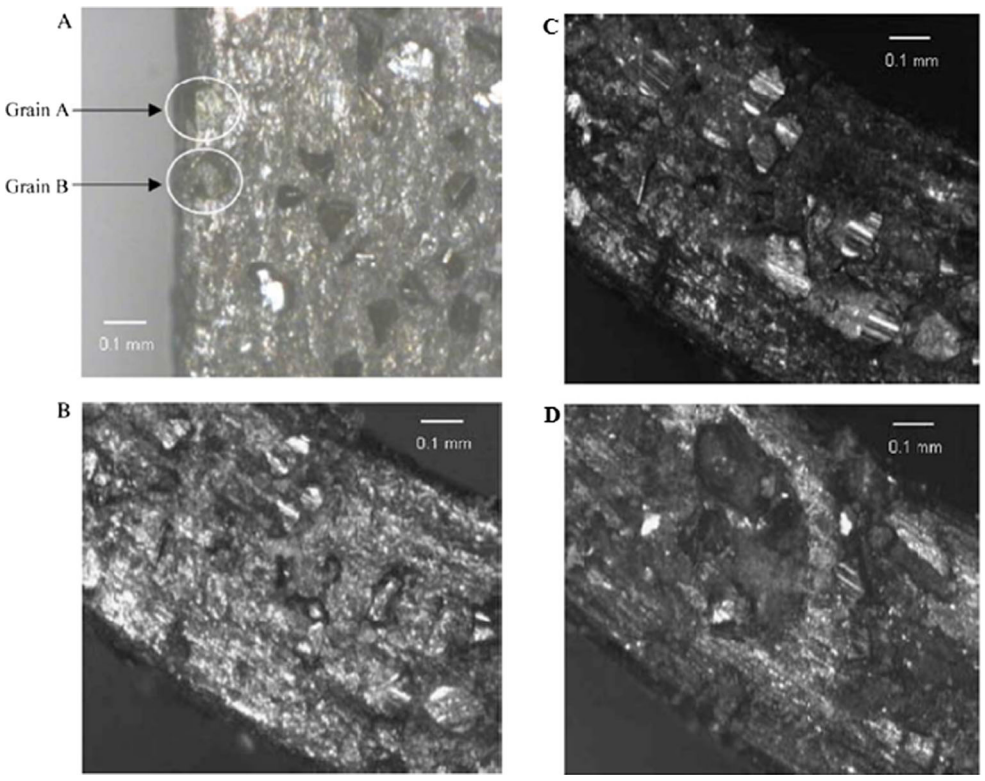

Fig. 2 Tool topography in SiC [3]

(a) Lateral face and (b) End Face before drilling test

(c) and (d) End Face after 6 and 16 drilling test

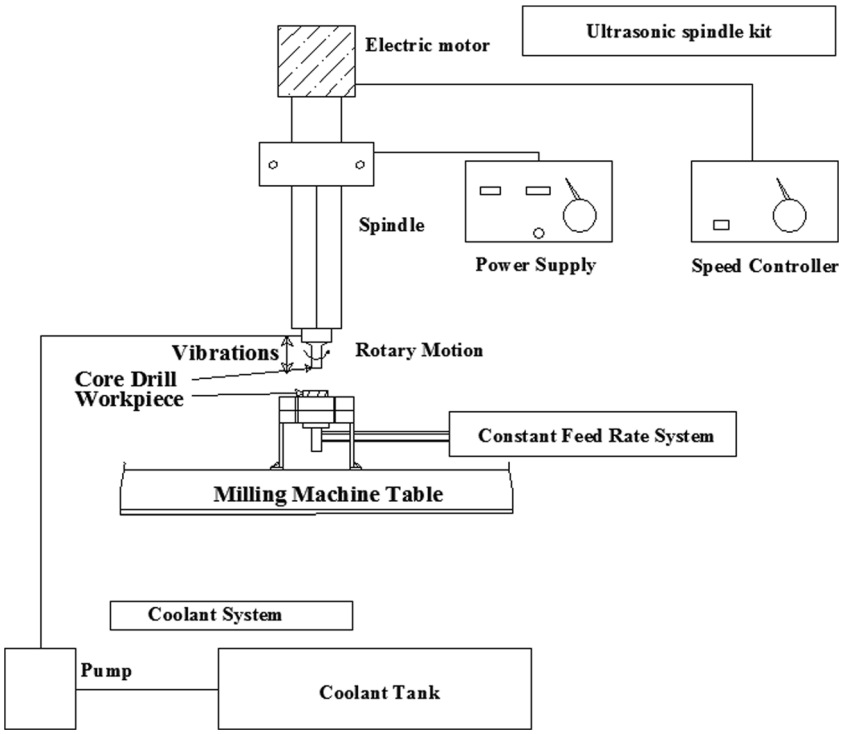

Fig. 3 Schematic diagram of RUM setup

bonded tools are more wear resistant, but these are very brittle. Hence, it is difficult to manufacture vitrified-bonded micro-tool. Metal-bonded tools are most wear resistant, as these are manufactured by sintering metal powder and diamond abrasive together [4]. Sintered tools have diamond particles in a matrix made of various metal combinations. Multiple layers of diamond are impregnated inside the metal matrix. Most of the electroplated tools have a single layer of diamonds, held by a tough durable nickel alloy on a steel body. Electroplated diamond products are able to retain their original shape and dimensions throughout their working life unlike sintered (metal bond) or resin bond diamond tools, where diamond particles are buried in the bond and held together by metal or resin binder. Electroplating allows diamond particles to protrude from the bond matrix, providing a free, fast cutting action with minimum heat generation [9, 10].

In RUM, hollow tool of different wall thickness, grain sizes were investigated by various researchers [6–8] for machining hard and brittle materials.

In the present study, tool wear was investigated by performing peck drilling operation using hollow geometry tools. Custom-made electroplated hollow geometry diamond tools were designed and realized through Sauer Germany. Sintered hollow diamond tools are not available due to manufacturing difficulties and hence not attempted in present study. Optical microscope and SEM images of new electroplated diamond tool of 300-μm outer diameter with 30-μm grain size and 100-μm wall thickness are shown in Fig. 5a, b.

(a) US50 Sauer Machine

(b) Ø300μm drilled hole while machining

Fig. 4 Experimental setup and Ø300-μm drilled hole while machining. **a** Microscope image of new tool at ×200. **b** SEM image of new tool at ×560

Fig. 5 Image of new tool

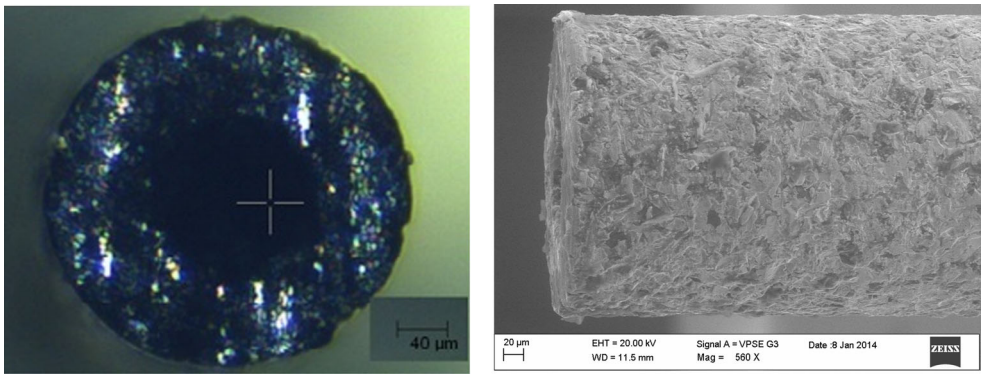

(a)Microscope image of new tool at 200X (b)SEM image of new tool at 560X

2.3 Experiment design and selection of process parameters

Design of experiment is a powerful tool for modeling and analyzing the effect of controllable factors on the performance output. Most prevailing classes of these designs are orthogonal first-order and central composite second-order designs [11]. First-order design is accepted over a narrow range of variables, whereas central composite design is used to predict a second-order behavior of the response for a wider range of process factors. Therefore, full factorial and central composite design techniques have been used in the present study in order to plan two different sets of experiments.

The central composite design technique is also called response surface methodology and yields the response as shown in Eq. (1).

$$Y = \beta_0 + \sum_{i=1}^{k} \beta_i X_i + \sum_{i=1}^{k} \beta_{ii} X_i^2 + \sum_{i<j} \sum \beta_{ij} X_i X_j + \varepsilon \qquad (1)$$

where "Y" represent the response variable; k is the number of variables; β_0, β_i, β_{ii}, and β_{ij} are the constant coefficients; and ε is the random error. X_i are factors or variables. The expression contains linear terms in X_i, quadratic terms in X_i^2, and product terms in X_iX_j representing the interaction effects.

In the present case, two sets of experimentation were conducted to evaluate the effect of μ-RUM parameters on specific tool wear for drilling operations. First set of experiment has been conducted to optimize the tool design-related parameter keeping process parameter constant, and second set of experiment has been conducted to optimize the process-related parameters using optimized tool that resulted from first set of experiments in μ-RUM mode.

First set of experimentation consisted of tool design-related parameters, i.e., grain size, thickness of tool, and concentration of abrasives. Micro-tool have smaller contact area; hence, for good profile cohesiveness, it is advisable to have higher concentration [10]. Abrasive concentration is defined as the weight of the abrasive in each cubic inch of the bond material. "When 72 karats of abrasive are added in 1 in^3 of bond material, then the abrasive concentration is called as 100 concentration" [8]. In the experiments, concentration (C) of abrasive grains was kept constant (C150) for all types of tool used. In the first set, four experiments were conducted at two levels of two factors (thickness of tool and grain size of tool) using full factorial design in μ-grinding and μ-RUM mode. Table 2 shows μ-grinding and μ-RUM tool parameters and levels used for experimentation.

The second set of experimentation consisted of process-related parameters, i.e., spindle speed, feed rate, distance traverse in each stroke for peck drilling also called depth of cut in present study, vibration amplitude, and vibration frequency using optimized tool from the first set of experiment. In second set, 33 experiments were conducted using central rotatable composite designs of experiments. Table 3 shows the μ-RUM process parameters and levels used for experimentation. These parameters and ranges were selected based on setup constraints, preliminary experimentation study, and literature review.

Borosilicate glass has been selected as workpiece material. The borosilicate glass has very low coefficient of thermal expansion, excellent bonding property, and surface integrity. These properties make borosilicate highly suitable for special applications in MEMS [12]. Micro-holes were required to be drilled in a micro-valve made of borosilicate glass (BK7) wafers for xenon gas delivery in space-related application. Therefore, drilling of Ø300-μm holes was selected for the experiment.

The first set of trial experiments was performed on 50-mm length, 50-mm width, and 1.4-mm thick size workpiece material. In each experiment, 10 numbers of holes were drilled for 1-mm depth in grinding and RUM mode. The various

Table 2 Levels of independent tool parameters for full factorial design

Factor representation	Description and unit	Levels	
		−1	1
Y_1	Grain size of diamond abrasive (μm)	15	30
Y_2	Wall thickness of hollow tool (μm)	80	100

Table 3 Levels of independent process factors for response surface design

Factor representation	Description and unit	Levels				
		−2	−1	0	1	2
X_1	Spindle speed (rpm)	2000	3000	4000	5000	6000
X_2	Feed rate (mm/min)	0.2	0.3	0.4	0.5	0.6
X_3	Distance traverse in each stroke (μm)	2	4	6	8	10
X_4	Vibration amplitude (percent of ultrasonic power)	50	62	74	86	98
X_5	Vibration frequency (kHz)	17.5	20.5	23.5	26.5	29.5

process parameters which were constant during these sets of experiments are given in Table 4. Table 5 shows the trials for first set of experimentation using full factorial and the corresponding response for μ-RUM and μ-grinding processes.

For the second set of experimentation, 100-mm length, 60-mm width, and 1.4-mm thick size of workpiece material was selected. For each experiment, 10 numbers of holes were drilled up to a depth of 1 mm. Optimized tool of 30-μm grain size and 100-μm wall thickness of Ø0.3 mm was used for this purpose. Table 6 shows the trial experimentation for second set of experiment using response surface methodology and response for μ-RUM process parameters.

In all the experiments, tool length was measured using Zoller tool presetter after each experiment as shown in Fig. 6. Before starting next experiment, tool was cleaned by dipping in acetone and reset within 10-μm radial runout and verified by 45X Zoller tool presetter for maintaining similar experiment conditions. Therefore, only longitudinal wear was found to be dominant. Here, lateral wear was not taken into account. Water-soluble cutting oil was used as external coolant with controlled pressure.

Generally, tool wear is defined as ratio of volume removed of tool to volume removed of workpiece. Performance index called grinding ratio denoted by G also called wear ratio or specific tool wear is used to characterize tool wear resistance in abrasive process such as USM, grinding, and RUM [5, 7, 13]. It is defined as the ratio of the volume of workpiece material removed to the volume of tool material removed [13] as specific tool wear is a direct indication of the material removed. In the present study, tool wear has been defined in terms of specific tool wear. Therefore, tool wear and specific tool wear are two different terms used in present study. In these experiments, volume of workpiece material removed was kept fixed. Since tool used was hollow and tool wear was measured for drilling operation, therefore, G was calculated as per Eq. (2).

$$G = \frac{\Delta V_{\text{workpiece}}}{\Delta V_{\text{tool}}} = \frac{\text{Number of drill holes} \times \text{Depth of drilled hole}}{\text{Initial length of tool} - \text{Final length of tool}} \quad (2)$$

3 Data analysis

Before analyzing the experimental data (Tables 5 and 6), a check for goodness of fit of the model is required. The model adequacy checking includes test for significance of the regression model, test for significance on model coefficients, and test for lack of fit. For the purpose, analysis of variance (ANOVA) has been performed.

3.1 Statistical modeling of specific tool wear as a function of μ-RUM tool design parameters

A model is derived using regression analysis to predict specific tool wear using data presented in Table 5. This model is presented below as Eq. (3). The obtained ANOVA of specific tool wear with confidence interval of 99 % is given as Table 7.

$$G = -180.0 + 1.30 \times Y_2 + 0.103 \times Y_1 \times Y_2 \quad (3)$$

where G denotes the specific tool wear, Y_1 is the grain size of diamond abrasive (μm), and Y_2 is the wall thickness of hollow tool (μm).

Table 4 μ-RUM and μ-grinding process parameters used for tool design experiment trial

Experiment condition	N (rpm)	f_r (mm/min)	d_p (μm)	A (percent of ultrasonic power)	f (kHz)
μ-grinding	3000	0.5	4	Off	Off
μ-RUM	3000	0.5	4	86	26.5

Table 5 Experiment trials and response for μ-RUM and μ-grinding to study the effect of tool design parameters on tool wear

Trial number	Grain size (μm)	Wall thickness (μm)	G (μ-RUM)	G (μ-grinding)
1	30	100	260	180
2	30	80	171	Tool break after two numbers of drilling
3	15	80	48	Tool break after six numbers of drilling
4	15	100	104	70

3.2 Statistical modeling of specific tool wear as a function of μ-RUM process parameters

The obtained model after analysis of data presented in Table 6 is to predict specific tool wear with confidence interval of 95 % by regression analysis presented by Eq. (4). The obtained ANOVA of G is given as Table 8.

$$\begin{aligned} G = & -3270.0 + 0.215 \times X_1 + 2451 \times X_2 \\ & + 109896 \times X_3 + 19.9 \times X_4 + 113 \times X_5 - 767 \\ & \times X_2 \times X_2 - 0.0912 \times X_4 \times X_4 - 1.86 \times X_5 \\ & \times X_5 - 0.235 \times X_1 \times X_2 - 0.00477 \times X_1 \\ & \times X_5 - 132533 \times X_2 \times X_3 - 938 \times X_3 \times X_4 \end{aligned} \quad (4)$$

where G denotes the specific tool wear, X_1 is the spindle speed (rpm), X_2 is the table feed rate (mm/min), X_3 is the distance traverse in each stroke (mm), X_4 is the vibration amplitude (percent of ultrasonic power) and X_5 is the vibration frequency (kHz).

4 Results and discussion

4.1 Comparison of μ-grinding and μ-RUM processes for specific tool wear

A comparative data analysis of specific tool wear for μ-grinding and μ-RUM for drilling of borosilicate glass using different tool geometries is presented in Table 5. Specific tool wear achieved in case of μ-RUM with 100-μm thickness, 15 and 30 grain size tools are 104 and 260, but in the case of μ-grinding, specific tool wear achieved are 70 and 180, respectively. It is inferred that minimum amount of specific tool wear can be improved by 44 % through μ-RUM as compared to μ-grinding process.

Catastrophic tool failures were observed for trials "2" and "3" in μ-grinding mode with 80-μm thickness tools, and the failure was observed after drilling of two and six numbers of holes, respectively, as shown in Fig. 7a, b. No tool break was observed while drilling in μ-RUM mode. It is inferred that for all four types of tools used in the experiments, RUM mode is most preferable for micro-machining over grinding with reduced tool wear. This may be because in RUM mode, tool contact with workpiece is intermittent, which allows heat to dissipate at faster rate and make chip evacuation better; hence, friction and contact stresses are less compared to grinding mode for brittle and hard material machining [14, 15].

4.2 Effect of μ-RUM tool design parameters on specific tool wear

The main effect plot, interaction plot, cube plot, and pie chart for specific tool wear were obtained using Minitab and Origin software and are shown in Figs. 8a, b and 9a, b. Figure 8a shows main effect of tool wall thickness on specific tool wear. It is inferred that wall thickness of electroplated tool is directly proportional to specific tool wear. In present study, increasing the wall thickness from 80 to 100 μm increases the specific tool wear from 110 to 180, i.e., an improvement of 63 %. Improvement in specific tool wear has been calculated for 100-μm thickness tool over 80-μm thickness tool, i.e., (180–110) × 100/110. The reason for increase of specific tool wear with increase in wall thickness may be because at higher wall thickness, tool can carry and withstand more cutting forces as compared to less wall thickness tool [8]. Carrying and withstanding higher cutting forces may allow less numbers of diamond particles to protrude from the bond matrix for higher wall thickness tool as compared to less wall thickness tool [10]. Thus, specific tool wear is more or tool wear is less for higher wall thickness tool.

Figure 8b shows interaction effect between wall thickness and grain size of tool on specific tool wear. It is inferred that for 80-μm wall thickness tool, specific tool wear increases from 48 to 171 as diamond grain size increases from 15 to 30 μm. Similarly, for 100-μm wall thickness tool, specific tool wear increases from 104 to 260 when grain size increases from 15 to 30 μm. It is observed that specific tool wear increases as grain size increases from 15 to 30 μm for both the thicknesses (80 and 100 μm) of tool. This is because for larger grain size, numbers of grain particles are less for constant contact surface area; hence, heat generation is less, and thus, tool wear is less or specific tool wear is more [5].

The cube plot is useful to design tool and shows the complete behavior of performance of the tool. For the

Table 6 Experiment trials and response to study the effect of μ-RUM process parameters on tool wear

Trial number	N (rpm)	f_r (mm/min)	d_p (mm)	A (percent of ultrasonic power)	f (kHz)	G
1	4000	0.4	0.006	74	23.5	166.66
2	3000	0.3	0.008	86	26.5	98.00
3	5000	0.3	0.008	62	26.5	173.91
4	3000	0.5	0.004	86	26.5	270.27
5	5000	0.3	0.004	62	20.5	105.26
6	4000	0.4	0.006	74	23.5	170.00
7	3000	0.5	0.004	62	20.5	130.96
8	3000	0.3	0.004	62	26.5	86.96
9	4000	0.4	0.006	74	23.5	165.00
10	5000	0.5	0.004	86	20.5	222.22
11	4000	0.4	0.006	74	23.5	153.84
12	3000	0.3	0.004	86	20.5	74.074
13	4000	0.4	0.006	74	23.5	158.64
14	5000	0.5	0.004	62	26.5	153.84
15	5000	0.5	0.008	62	20.5	80.00
16	5000	0.3	0.004	86	26.5	181.81
17	4000	0.4	0.006	74	23.5	181.81
18	3000	0.3	0.008	62	20.5	68.96
19	5000	0.3	0.008	86	20.5	142.85
20	5000	0.5	0.008	86	26.5	76.92
21	3000	0.5	0.008	62	26.5	157.82
22	3000	0.5	0.008	86	20.5	74.07
23	4000	0.4	0.006	74	17.5	30.14
24	4000	0.4	0.006	74	23.5	137.93
25	4000	0.4	0.01	74	23.5	100.38
26	4000	0.4	0.006	98	23.5	105.26
27	2000	0.4	0.006	74	23.5	135.90
28	4000	0.2	0.006	74	23.5	115.13
29	6000	0.4	0.006	74	23.5	160.00
30	4000	0.4	0.006	50	23.5	86.96
31	4000	0.6	0.006	74	23.5	120.76
32	4000	0.4	0.006	74	29.5	133.33
33	4000	0.4	0.002	74	23.5	224.72

experiments, cube plot has been shown in Fig. 9a. Tool having 100-μm wall thickness with 30-μm grain size is seen to be the most promising (optimized) tool for machining micro-feature with maximum specific tool wear.

The pie chart as shown in Fig. 9b has been plotted to display percentage contribution of significant factors on specific tool wear. From pie diagram, it can be concluded that interaction factor between grain size and thickness contribute maximum (77 %) effect on specific tool wear followed by thickness of tool is 23 %.

4.3 Effect of μ-RUM process parameters on specific tool wear

The percentage contribution of significant factors is shown in Fig. 10 using pie chart.

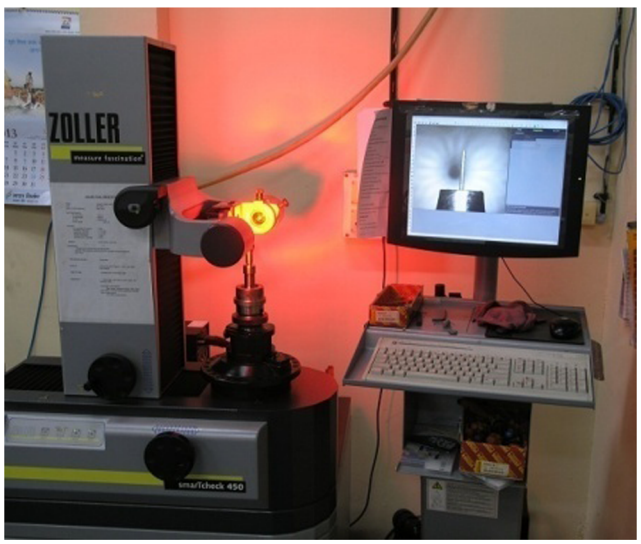

Fig. 6 Tool presetter

Table 7 Analyses of variance of first set of experiment

Source	*df*	Seq. SS	MS	*F*	*P*	R^2 (%)	
Regression	2	24,988	12,494	12,648.13	0.006	99.99	$F^{\text{standard}}_{(0.01,2,1)} = 4,999.5$
Residual error	1	1	1				$F^{\text{regression}} > F^{\text{standard}}_{(0.01,2,1)}$
Total	3	24,989					Model is adequate and lack of fit is insignificant

Figure 11a–e shows main effect plot for specific tool wear. Figures 12, 13, 14, and 15 show the interaction effect plots for specific tool wear.

4.3.1 Main effects

Pie diagram was plotted to display percentage contribution of significant factors on specific tool wear as shown in Fig. 15. From pie diagram, it was found that depth of cut (18 %) and vibration frequency (13 %) are major factors affecting specific tool wear linearly. Vibration frequency has a quadratic affect (10 %) on specific tool wear. Depth of cut and feed (13 %), spindle speed and feed (10 %), followed by depth of cut and vibration amplitude (9.6 %) are the major interaction factors influencing specific tool wear.

The effect of feed rate on specific tool wear is shown in Fig. 11b. It is inferred that at smaller feed rates of 0.2 and 0.3 mm/min, specific tool wear is less. Here, the friction between tool and workpiece may be the dominating factor, which implies that minimum feed rate should be maintained for drilling operation to have minimum tool wear. Specific tool wear increases from 120 to 147 with increase of feed rate from 0.3 to 0.5 mm/min and then decreases for a feed rate of 0.5 to 0.6 mm/min. This is due to fact that at this feed rate of 0.3–0.5 mm/min, heat dissipation effects dominate over contact/friction between tool and workpiece. At 0.6-mm/min feed rate, tool undergoes rapid wear due to high load on tool [8, 16].

The effect of spindle speed on specific tool wear is shown in Fig. 11a. It is inferred that with increase of spindle speed from 3000 to 6000 rpm, specific tool wear increases from 120 to 170. This is because increase in spindle speed results in reduced cutting time as well reduced cutting forces [8], which in turn reduces the propagation of wear by dissipating heat and inducing less stresses. Thus, tool wear is less.

The effect of depth of cut on specific tool wear is shown in Fig. 11c. It is inferred that with increase of depth of cut from 2 to 10 μm, specific tool wear decreases from 225 to 100. This is because as the depth of cut increases, mechanical load between tool and workpiece increases, thus allowing diamond particles to protrude from bond matrix [5, 16]. It is observed that at lower depth of cut (2 μm), specific tool wear is very high. This may be because at 2-μm depth of cut, mechanical load experienced by tool is very less and results in minimum tool wear.

The effect of vibration amplitude on specific tool wear is shown in Fig. 11d. It is seen that with increase in vibration amplitude from 50 to 86 %, specific tool wear increases from 85 to 125 and decreases from 125 to 95 for vibration amplitude of 86 to 98 %. Hence, for each tool setup, vibration amplitude should be set for minimum tool wear.

The effect of vibration frequency on specific tool wear is shown in Fig. 11e. It is inferred that vibration frequency increases from 17.5 to 26.5 kHz, specific tool wear first increases from 30 to 150, and then decreases from 150 to 130 for frequency of 26.5 to 29.5 kHz. It is observed that at very low frequency (17.5 kHz), specific tool wear is very low (30). This may be because in micro-machining, amplitude of vibration is small, and at the low ultrasonic frequency, the vibration energy may not be sufficient to prevail ultrasonic effect, thus acting like grinding.

4.3.2 Interaction effect

The interaction effect between depth of cut and vibration amplitude on specific tool wear is shown in Fig. 12. From 74 to 98 % vibration amplitude range, specific tool wear decreases

Table 8 Analyses of variance of *G* for μ-RUM process parameters

Source	*df*	Seq. SS	Adjusted MS	*F*	*P*	R^2	
Regression	12	78,162	6,513.5	21.54	0.001	92.82 %	$F^{\text{standard}}_{(0.05,12,20)} = 2.28$
Linear	5	32,409					$F^{\text{regression}} > F^{\text{standard}}_{(0.05,12,20)}$
Square	3	14,295					
Interaction	4	31,458					$F^{\text{standard}}_{(0.05,14,20)} = 2.22$
Residual error	20	6,047	302.4				$F^{\text{lack of fit}} < F^{\text{standard}}_{(0.05,14,20)}$
Lack of fit	14	4,903		1.84	0.234		
Pure error	6	1,145					Model is adequate and lack of fit is insignificant
Total	32	84,209					

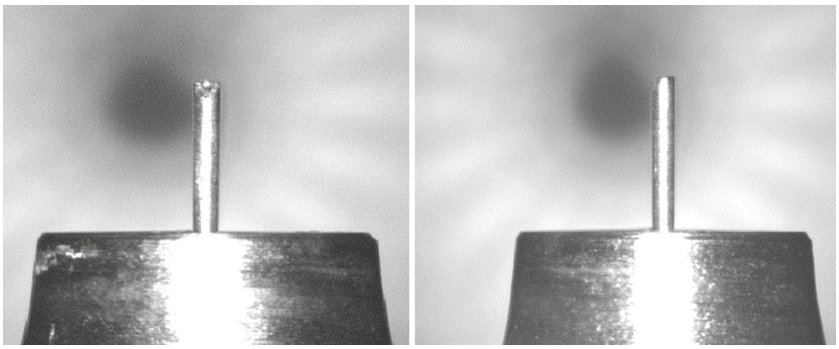

(a) Tool break in grinding mode in trial 2(first set of expt.)

(b) Tool break in grinding mode in trial 3(first set of expt.)

Fig. 7 Broken tool image using tool presetter in μ-grinding mode

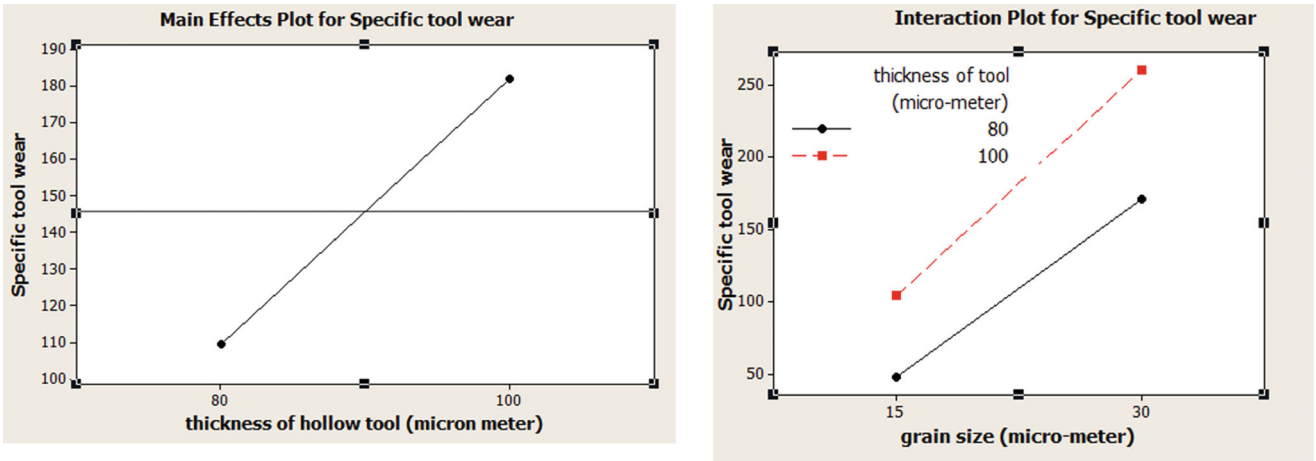

(a) Main effect plot for G

(b) Interaction plot for G

Fig. 8 Main effect and interaction plot for specific tool wear

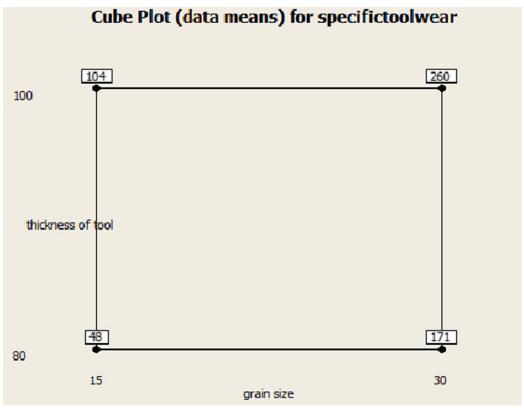

(a) Cube effect plot for G

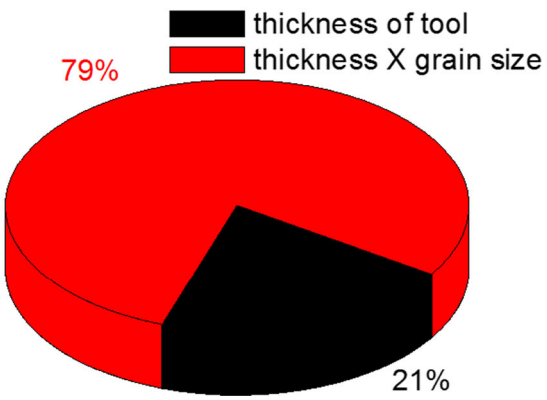

(b) Pie diagram showing % contribution of significant factors on G

Fig. 9 Cube plot and pie diagram for specific tool wear

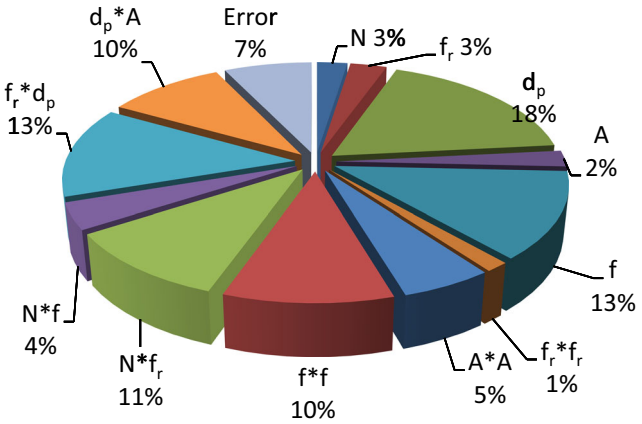

Fig. 10 Pie diagram showing percent contribution of significant factors on G

with increases in depth of cut. This may be because at high value of vibration amplitude, effect of mechanical load/stress is dominant as depth of cut increases. From 50 to 74 % range of amplitude, specific tool wear increases with increase in depth of cut initially, then becomes constant. This may be because at low value of vibration amplitude, heat dissipation rate is dominant as depth cut increases.

The interaction effect between feed rate and depth of cut on specific tool wear is shown in Fig. 13. It is inferred that from 0.4 to 0.6 mm/min feed rate range, specific tool wear decreases with increase in depth of cut. This may be because at high value of feed, the effect of mechanical load is dominant as depth of cut increases. From 0.2- to 0.4-mm/min feed rate range, specific tool wear increases with increase in depth of cut initially, then be-

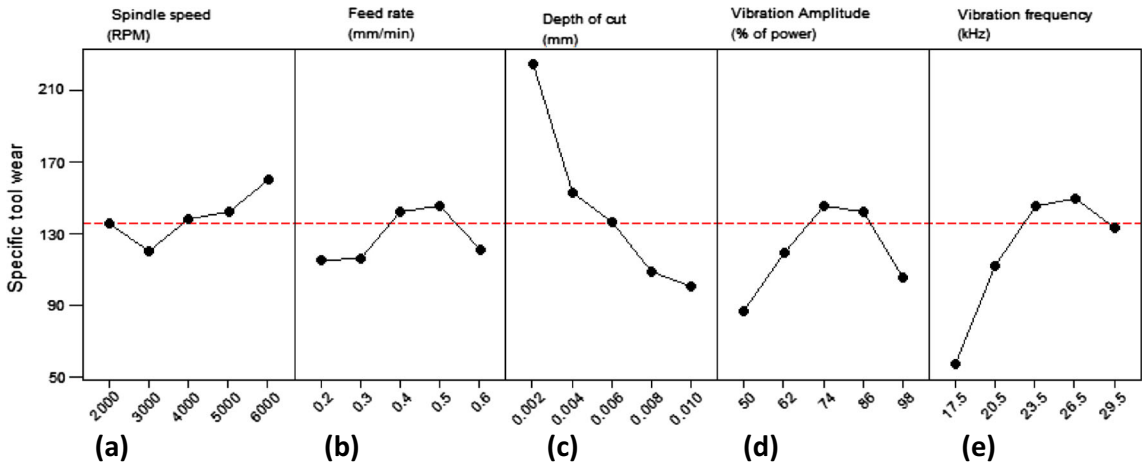

Fig. 11 Main effect plot

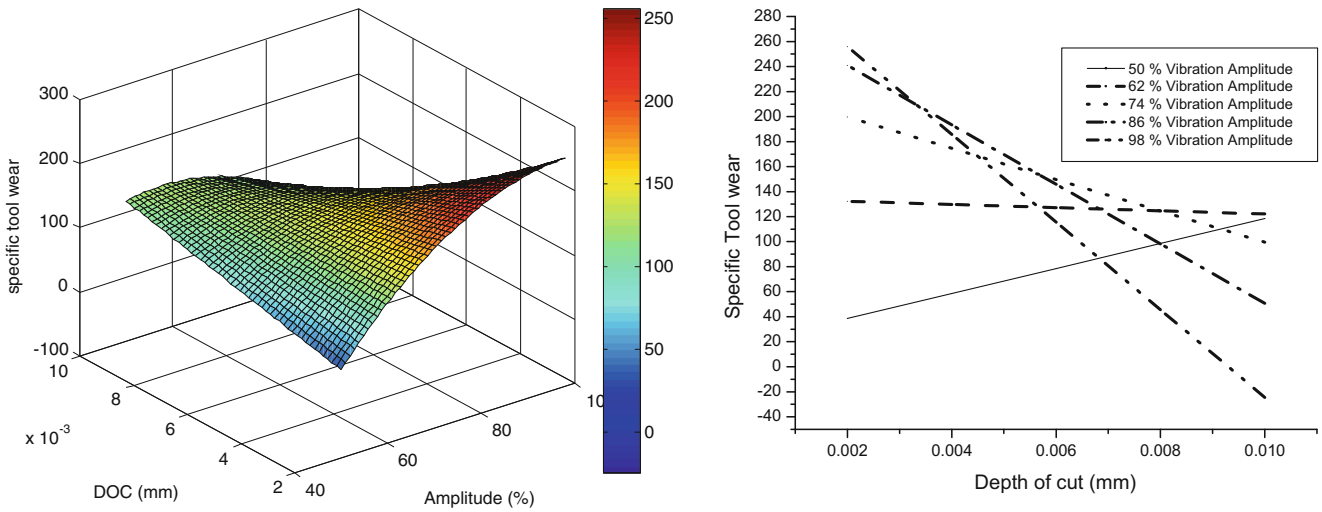

Fig. 12 Interaction effect between d_p and A **a** response surface for G and **b** variation of G with d_p and A ($N = 4000$ rpm, $f_r = 0.4$ mm/min, and $f = 23.5$ kHz are fixed)

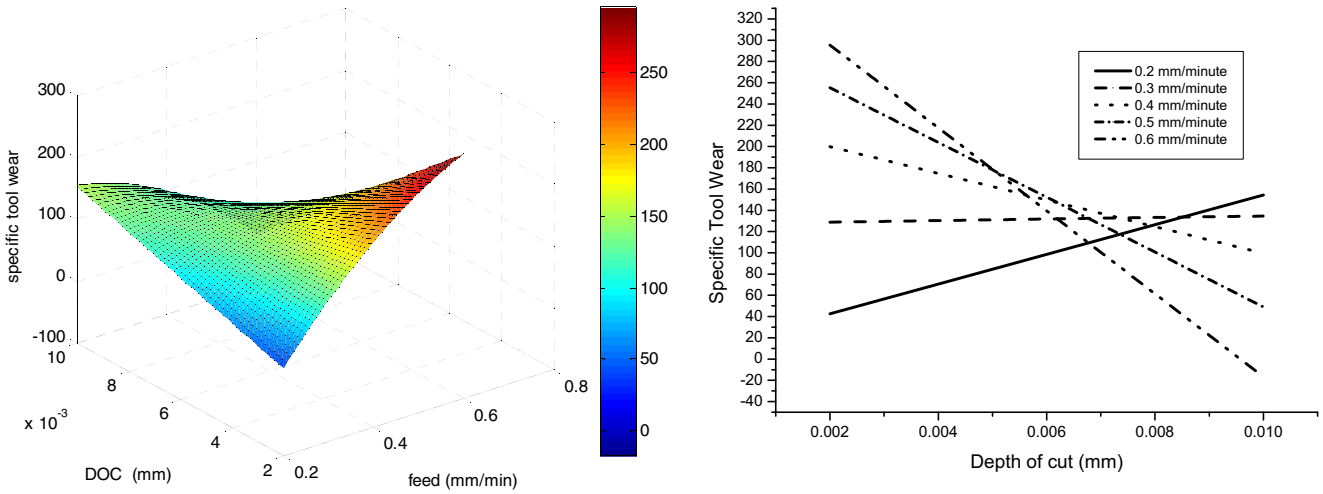

Fig. 13 Interaction effect between d_p and f **a** response surface for G and **b** variation of G with d_p and f_r ($N = 4000$ rpm, $A = 74$ %, and $f = 23.5$ kHz are fixed)

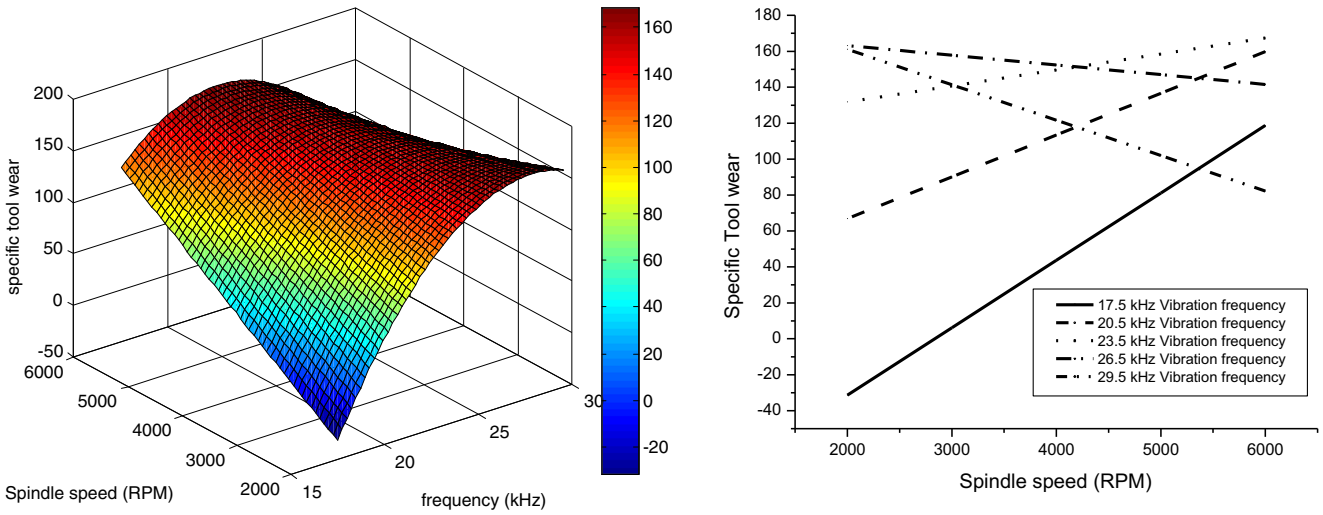

Fig. 14 Interaction effect between f and N **a** response surface for G and **b** variation of G with f and N ($A = 74$ %, $f_r = 0.4$ mm/min, and $d_p = 0.006$ mm are fixed)

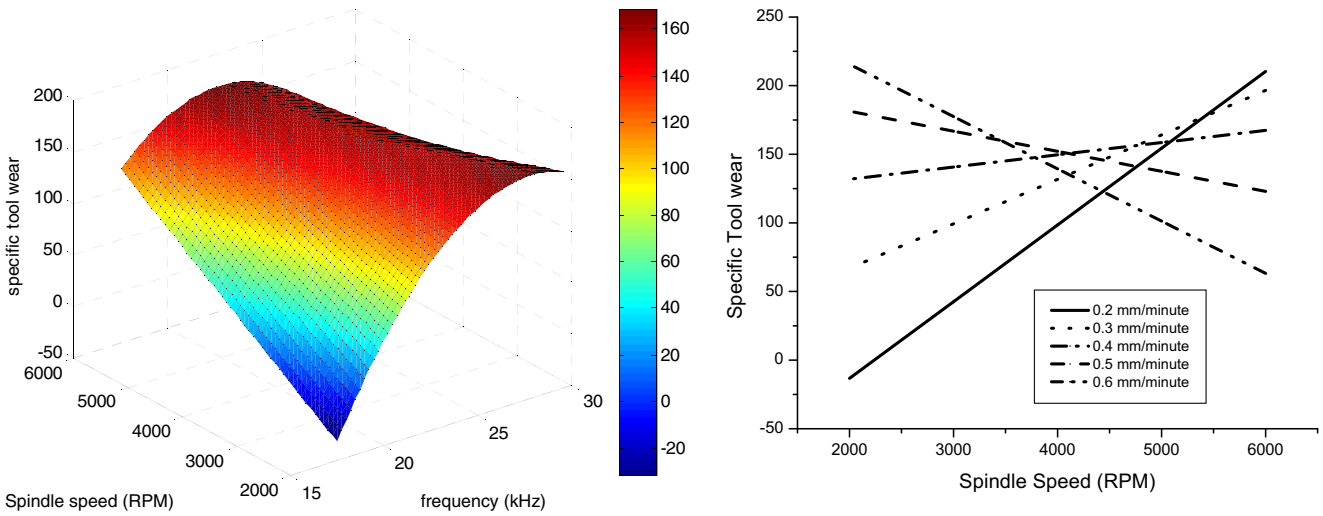

Fig. 15 Interaction effect between N and f **a** response surface for G and **b** variation of G with N and f_r ($A = 74$ %, $f = 23.5$ kHz, and $d_p = 0.006$ mm are fixed)

Table 9 Confirmation experiments for μ-RUM tool design parameter

Serial number	Drilling conditions		*G*	
	Grain size (μm)	Wall thickness (μm)	As predicted by Eq. (5)	Obtained in experiments
1	15	80	43 ± 5.84	47.6
2	30	100	251 ± 5.84	256.8
3	15	100	95 ± 5.84	100.5

comes constant. This may be because at low range of feed rate, load/stress experienced by the tool was less.

The interaction effect between vibration frequency and spindle speed on specific tool wear is shown in Fig. 14. It is inferred that from 17.5- to 23.5-kHz vibration frequency range, specific tool wear increases with increase in spindle speed. This may be because at this range of vibration frequency, force experienced by tool decreases as spindle speed increases. From 23.5- to 29.5-kHz vibration frequency range, specific tool wear become constant initially, then decreases marginally with increase of spindle speed. The 26.5-kHz vibration frequency may be the resonance frequency of tool, and beyond resonance frequency, transmission of ultrasonic energy marginally decreases; thus, average forces/stresses on tool may be little high.

The interaction effect between feed rate and spindle speed on specific tool wear is shown in Fig. 15. It can be seen that from 0.2- to 0.4-mm/min feed rate range, specific tool wear increases with increase in spindle speed. This may be because at low range of feed rate, tool wear decreases with increase of spindle speed as force on tool was less. From 0.4- to 0.6-mm/min range of feed rate, specific tool wear becomes constant initially, then decreases with increase in spindle speed. This may be because at value of high range of feed rate, force induced on tool was high.

5 Validation

5.1 Precision of the predictive model

Due to experimental error, estimated change in specific tool wear is subjected to uncertainty. The precision of specific tool wear was estimated by calculating confidence interval. The confidence interval for the predicted response is $G \pm \delta(G)$, where $\pm\delta(G)$ is given by Eq. (5).

$$\delta(G) = t_{\alpha/2,\ df} \times \sqrt{V_e} \tag{5}$$

Here, $t_{\alpha/2,df}$ is the value of horizontal coordinate on t distribution corresponding to specific degrees of freedom (df), α is the level of confidence interval, and V_e is the variance of error of the predictive model. $\delta(G)$ value for surface was calculated using the values of error variance from Tables 7 and 8. The values of α have been taken as 0.01 and 0.05, respectively. The values of $\delta(G)$ were calculated as ±5.84 and ±35.3.

For validating the predictive models, a few experiments (other than Tables 5 and 6) were carried out and the details are provided in Tables 9 and 10. It can be concluded that the experimental values of G are within the range predicted by the two statistical models.

6 Factor setting for maximum specific tool wear

6.1 Optimum process parameters for maximizing specific tool wear

In order to estimate the best performance of the μ-RUM process for borosilicate glass, the objective functions given by Eq. 4 have been optimized using trust region method toolbox available in MATLAB software. For the validation, an experiment was performed at the factor setting at which the model was maximized. The value obtained was between lower and upper limits (confidence interval) and has been presented in Table 11.

7 Conclusions

Following conclusion were made by above study:

1. Comparative study between μ-RUM and μ-grinding for specific tool wear was carried out by performing drilling operation in borosilicate glass for different types of tool geometry using electroplated diamond tool of Ø300 μm.

Table 10 Confirmation experiments for μ-RUM process parameter

Serial number	Drilling conditions					*G*	
	N (rpm)	f_r (mm/min)	d_p (mm)	*A* (percent of ultrasonic power)	*f* (kHz)	As predicted by Eq. (5)	Obtained in experiments
1	4000	0.4	0.006	74	23.5	170 ± 35.3	149.62
2	4000	0.4	0.006	74	17.5	35 ± 35.3	43.66
3	4000	0.5	0.006	50	23.5	93 ± 35.3	81.06
4	400	0.5	0.004	74	26.5	190 ± 35.3	206.50

Table 11 Optimum μ-RUM process parameter

Serial number	Drilling condition					Specific tool wear	
	N (rpm)	f_r (mm/min)	d_p (mm)	A (percent of ultrasonic power)	f (kHz)	As predicted	Obtained in experiments
1	4000	0.5	0.002	86	26.5	299.2 ± 35.3	275

Minimum amount of specific tool wear can be increased to 44 % in μ-RUM compare to μ-grinding.

2. Two-factor two-level factorial design of experiment was used for tool-related parameters in μ-RUM. It was found that the main effect of thickness and interaction effect between grain size and thickness have direct impact on specific tool wear. It is observed that specific tool wear was improved by 63 % as thickness of tool increased from 80 to 100 μm. It is also seen that for 100-μm thickness tool, specific tool wear improved by 150 % as grain size increased from 15 to 30 μm.
3. Tool design parameters (grain size and thickness) were optimized through cube plot and found that tool having 100-μm thickness with 30-μm grain size to be most promising tool for drilling operation with maximum specific tool wear. Using this tool, effect of μ-RUM process parameters on specific tool wear were investigated using five-level five-factor central rotatable composite designs of experiments.
4. Specific tool wear was directly proportional to rotational speed. Specific tool wear was constant for 0.2–0.3-mm/min feed rate range, then start increasing for 0.3–0.5-mm/min feed rate range, and finally decreases after attaining 0.5-mm/min feed rate. Specific tool wear decreases as depth of cut increases. Specific tool wear increases with increase in vibration amplitude and vibration frequency up to certain value, then starts decreasing.
5. Vibration frequency was the most influencing parameter on tool wear. It was found that at 17.5-kHz vibration frequency, specific tool wear was very low or tool wear was very high.
6. Confirmatory experiments were conducted and found accurate within 99 and 95 % confidence intervals for tool- and process-based parameters.
7. μ-RUM process parameters were optimized for 100-μm thickness and 30-μm grain size tool for maximum specific tool wear (299.25).

Acknowledgments The authors gratefully acknowledge the financial support provided by Shri Koshy M. George, Deputy Director, MME, and Shri Shibu Gopinath, GM, IFF, to acquire custom-made electroplated micro-tool. Authors also express their thankfulness to Kasala Narasaiah, Deputy General Manager, AMF, to spare rotary ultrasonic machine and other resources for carrying out this work.

References

1. Hu P, Zhang JM, Pei ZJ (2003) Experimental investigation on coolant effects in rotary ultrasonic machining, NSF Workshop on Research Needs in Thermal Aspects of Material Removal Processes, Stillwater, OK, pp. 1–6
2. Kiran RS Kolluru VSS (2005) Rotary ultrasonic machining—a review, Proceeding of National Aerospace Manufacturing Society, 22–23, pp.105–114
3. Kumar J, Khamba JS (2009) Investigating the machining characteristics of titanium using ultrasonic machining. A PhD Thesis Thapar University of Patiala
4. Feng J (2010) Micro grinding of ceramic materials, PhD Thesis University of Michigan
5. Pei ZJ, Khanna N, Ferreira PM (1995) Rotary ultrasonic machining of structural ceramics: a review. Ceram Eng Sci Proc 16:259–27
6. Churi N (2010) Rotary ultrasonic machining of hard to machine material, PhD Thesis University of Kansas State
7. Zeng WM, Li ZC, Pei ZJ, Treadwell C (2005) Experimental observation of tool wear in rotary ultrasonic machining of advanced ceramics. Int J Mach Tools Manuf 45:1468–1473
8. Qin N (2011) Modelling and experimental investigations on ultrasonic vibration assisted grinding Phd Thesis University of Kansas State
9. Park WH (2008) Development of micro-grinding mechanics and machine tools, PhD Thesis, Georgia Institute of Technology
10. www.glidemeiseister.com/de/ultrasonic/Sauer diamond tool catalogue
11. Montgomery (2001) Design and analysis of experiments. Wiley (Asia), Singapore. DC
12. Rakesh S, Kiran Kolluru VSS (2009) Micro-hole drilling in Pyrex wafer for high pressure micro valve application. National Conference on Expanding Frontiers in Propulsion Technology ASET
13. Malkin S (2006) Grinding technology theory and applications of machining with abrasives, Society of Manufacturing (SME) Press
14. Gong H, Fang FZ, Hu XT (2010) Kinematic view of tool life in rotary ultrasonic side milling of hard and brittle materials. Int J Mach Tools Manuf 50(3):303–307
15. Lv D, Huang Y, Wang H, Tang Y, Wu X (2013) Improvement effects of vibration on cutting force in rotary ultrasonic machining of BK7 glass. J Mater Process Technol 213(9):1548–1557
16. Sivasakthivel PS, Vel Murugan V, Sudhakaran R (2010) Prediction of tool wear from machining parameters by response surface methodology in end milling. Int J Eng Sci Technol 2(6):1780–1789